Th. G. Brown, K. Creath, H. Kogelnik,
M. A. Kriss, J. Schmit, M. J. Weber (Eds.)

WILEY-VCH

The Optics Encyclopedia

Basic Foundations
and Practical Applications

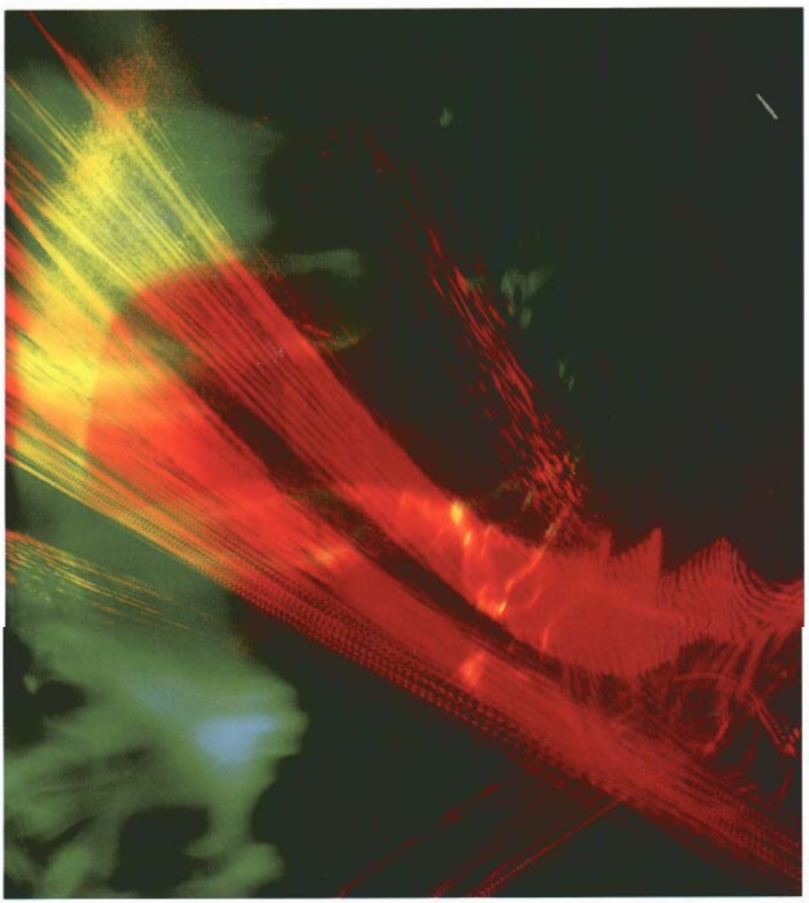

Volume 2
G–L

Lidar (Laser Radar)

P. S. Argall and R. J. Sica
Department of Physics and Astronomy, The University of Western Ontario, London, Ontario, Canada, N6A 3K7
Phone: (519) 661-2111 x86554; Fax: (519) 661-2111; e-mail: sargall@physics.uwo.ca

Abstract
Lidar is an active remote sensing technique similar in principle to radar, except that it utilizes light rather than radio waves. Lidar finds applications in many areas, including atmospheric and oceanic research, digital mapping, chemical and biological agent detection, speed measurement, and targeting. This chapter describes the principles of lidar and provides examples of the application of lidar in measuring the properties of the Earth's atmosphere.

Keywords
lidar; laser–radar; laser; atmospheric optics; Rayleigh; aerosol; DIAL; Raman.

1 Introduction

Lidar (light detection and ranging) is an active optical technique in which a beam of light is used to make remote range-resolved measurements. A lidar emits a light beam that interacts with the medium or object under study; some of this light is scattered back and detected by the lidar. Analysis of the backscattered light allows some property of the medium or object to be determined.

The major scientific use of lidar is in the measurement of the properties of the Earth's atmosphere, while the major commercial uses of lidar are aerial surveying and bathymetry (water depth measurement). Lidar also finds extensive application in ocean research, forestry, and biomass research; it has numerous other applications including chemical and biological agent detection and vehicle speed measurement. Lidar-equipped binoculars are used by hunters and golfers for range finding, while imaging lidar is beginning to find applications in producing 3-D electronic representations of objects, such as buildings, for virtual reality applications.

2 Historical Overview

Synge [1] first proposed the method of determining atmospheric density by the detection of scattering from a beam of light projected into the atmosphere in 1930. Synge suggested a scheme in which an antiaircraft searchlight could be used as the source of the beam and a large telescope with photoelectric apparatus for detection of the scattered light. Ranging, determining the distance at which the scatter occurred, could be accomplished by operating in a bistatic configuration with the source and receiver separated by several kilometers, Fig. 1.

The first reported results obtained using the principles of this method are those of Duclaux [2] who made a photographic recording of the scattered light from a searchlight beam. The transmitted beam was visible on the photograph to an altitude of 3.4 km. Hulbert [3] extended these results in 1936 by photographing a beam to a 28-km altitude.

A monostatic lidar, the typical configuration of modern lidars, has the transmitter and receiver colocated, Fig. 1. Monostatic lidars use a pulsed light source and measure the round-trip time of the scattered light pulses to enable ranging, Fig. 2. The first reported use of a monostatic lidar was by Bureau [4] in 1938; this system was used for measuring cloud base heights.

In 1956, Friedland et al. [5] reported the first pulsed monostatic system for atmospheric density measurements. A pulsed monostatic lidar allows each light pulse fired to provide a complete

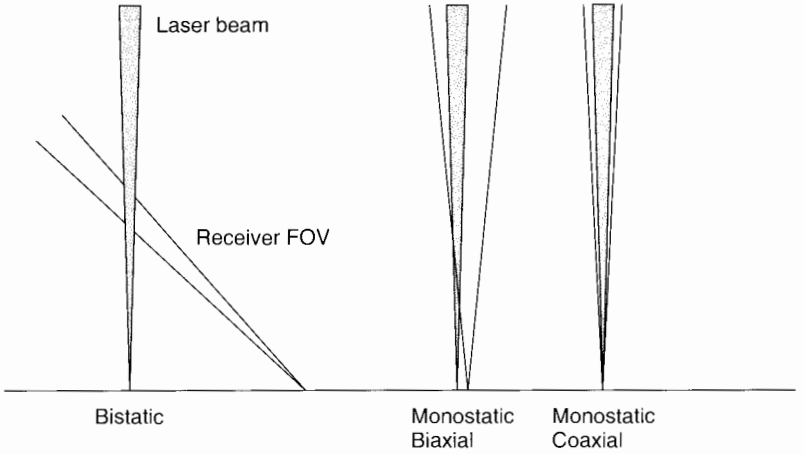

Fig. 1 Geometric arrangements of lidar transmitter and receiver

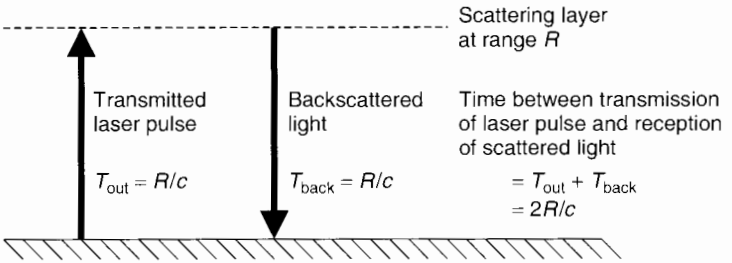

Fig. 2 Relationship between backscatter interval and range

altitude-scattering profile; a bistatic system requires the alignment of the laser and the detector field-of-view (FOV) to be changed so that an altitude profile can be obtained. Although a monostatic lidar records a complete altitude profile for each pulse fired, commonly, many such profiles are required to obtain measurements with a useful signal-to-noise ratio (SNR).

The invention of the laser [6] in 1960 and the pulsed laser [7] in 1962 provided a powerful new light source for lidar systems. Since the invention of the laser, developments in lidar have been closely linked to advances in laser technology. The first use of a laser in a lidar system was reported in 1962 by Smullins and Fiocco [8], who detected laser light scattered from the lunar surface using a ruby laser that fired 0.5-J pulses at 694 nm.

3 Lidar Basics

A lidar instrument can be conveniently divided into three subsystems: the transmitter, the receiver, and the detector. Each of these subsystems is discussed in the following sections in the context of an atmospheric lidar. Figure 3, a block diagram of a generic lidar system, shows how these subsystems fit together to form a complete lidar.

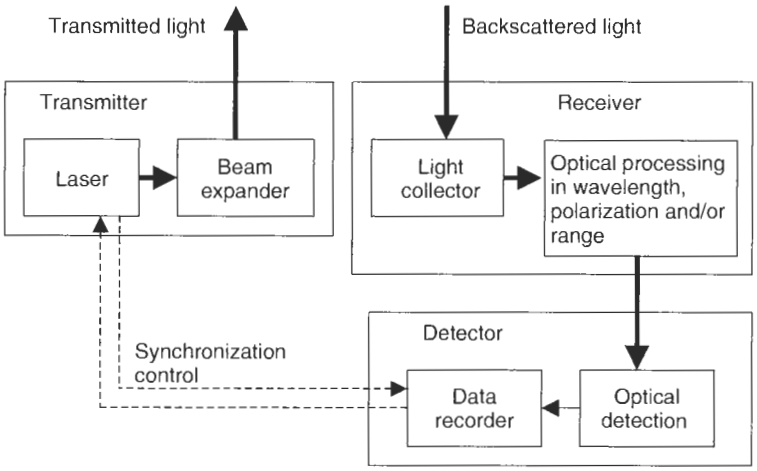

Fig. 3 Schematic of a simple lidar

3.1 Transmitter

The transmitter of a lidar is the subsystem that generates light pulses and directs them into the atmosphere. Figure 4 shows the laser beam of the University of Western Ontario's Purple Crow Lidar against the night sky. Because of the special characteristics of the light they produce, pulsed lasers are ideal as the sources for lidar systems. Three properties of a pulsed laser – low beam divergence, extremely narrow spectral width, and short intense pulses – provide significant advantages over white light as the light source for a lidar.

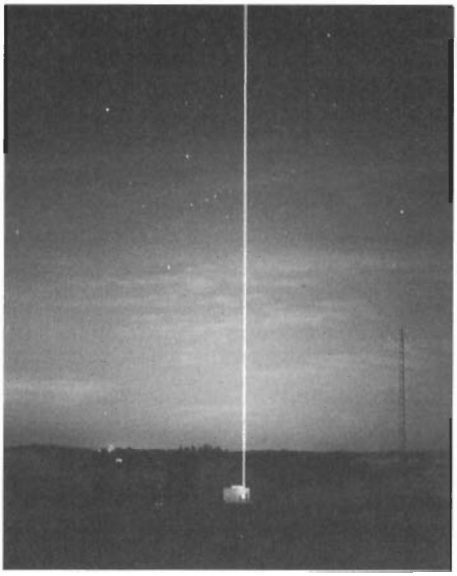

Fig. 4 The University of Western Ontario's Purple Crow Lidar operating at night. The sky near the horizon is illuminated by the sun

For most lidar systems, it is advantageous to have a transmitted beam with low divergence. The FOV of the detection system is one of the factors affecting the level of the background, measured scattered sunlight, moonlight, starlight, and so on in lidar measurements. A smaller FOV leads to a smaller measured background. Most lidars require that the transmitted laser beam be within the FOV of the detection system, thus a low FOV requires a low divergence laser beam. Many lidar systems incorporate a beam expander to reduce the divergence of the laser beam before transmission.

The inherent narrow spectral width of the laser has been used to advantage in many different ways in lidar. The simplest of these methods involves the spectral filtering of the backscattered light to reduce the background. Transmitting a beam with a narrow spectral width allows the detection optics of a lidar to spectrally filter incoming light and thus, selectively transmit photons at the laser wavelength. In practice, a narrowband interference filter is used; this transmits a relatively large fraction of the scattered laser light while transmitting only a very small fraction of background white light. This spectral selectivity allows the signal-to-background ratio of the measurement to be many orders of magnitude greater when a narrowband source and a detector system interference filter are used in a lidar.

The inherent pulsed properties of some types of laser systems make them ideal light sources for lidar; they allow ranging to be achieved by timing the scattered signal, Fig. 2. Other properties of the pulsed laser, namely, the pulse-repetition-frequency (PRF) and the pulse length, can have an influence on the operation of a lidar. The aliasing range of a lidar is the distance a laser pulse travels before the next pulse is transmitted. Usually, a lidar operates with a PRF such that at any time, no two pulses are within the range that causes scattering, that is, the aliasing range is much greater than the scattering range. The spatial length of the transmitted laser pulses ultimately limits the spatial resolution of the lidar measurements.

The type of laser used in a lidar system depends on the physical quantity the lidar is to measure. Some measurements require a very specific wavelength (i.e., resonance–fluorescence) or wavelengths (i.e., differential absorption lidar, DIAL) and can require complex laser systems to produce these wavelengths. Other lidars can operate over a wide wavelength range (i.e., Rayleigh, Raman, and aerosol lidars). The power, PRF, pulse length, and spectral width of a laser must also match the requirements of the measurements.

3.2 Receiver

The receiver of a lidar collects and processes the scattered laser light and then directs it to a photodetector. The primary optic in a lidar receiver is the optical element that collects the light scattered back from the atmosphere. Along with the power of the laser, the size of the primary optic is an important factor in determining the effectiveness of a lidar system. A larger primary optic will collect a greater fraction of the scattered light and thus increase the signal measured by the lidar. The size of the primary optics used in lidars varies from about 10 cm, usually refractive systems, up to a few meters in diameter, usually reflective components. The smaller aperture optics are used in lidar systems that are designed to work at close range, for example, a few 100 m. Larger aperture primary optics are used in lidar systems that are designed to probe the middle and upper regions of the Earth's atmosphere in which the returned signal is a much smaller fraction of the transmitted power.

After collection by the primary optic, the backscattered light is usually processed in some way before being directed to the detector system. This processing can be based on wavelength, polarization, and/or range depending on the purpose for which the lidar has been designed.

The simplest form of spectral filtering is the use of a narrowband interference filter tuned to the laser wavelength. This is used to significantly reduce the background,

as described in Sect. 3.1. More complex spectral filtering schemes are used for Doppler and high spectral resolution lidar [9–13]. These techniques require the measurement of spectral properties of the backscattered light.

Lidars used to study atmospheric aerosols and clouds often incorporate signal separation schemes based on the polarization of the backscattered light [14, 15] to obtain information about the scatterers, see Sect. 5.

Processing of the backscattered light based on range is usually performed in order to protect the detector from the intense near-field returns experienced by higher-power lidar systems. Exposing a photomultiplier (PMT) to a bright source such as near-field returns, even for a very short time, produces signal-induced noise, which affects the ability of the detection system to accurately record subsequent signals [16, 17]. Protecting the detector from these near-field returns can be achieved in a number of ways. One way is to use either a mechanical or electro-optical chopper that closes the optical path to the detector during and immediately after the laser fires. Another method involves removing the potential difference between two dynodes near the front of the PMT, effectively turning it off while the laser is fired; this technique is called *gating*.

3.3 Signal Detection and Recording

The signal detection and recording section of a lidar is that part of the instrument that takes the light from the receiver system and produces a permanent record of the backscattered intensity, and possibly wavelength and/or polarization, as a function of altitude. In the first lidar experiments, signal detection and recording was achieved using a photographic film [2, 3].

In modern lidars, detection and recording is achieved electronically. The detector converts the light into an electrical signal and the recorder is an electronic device or devices that process and store the electrical signal.

Photomultiplier tubes (PMTs) are generally used as detectors for incoherent lidar systems operating with visible or UV light. PMTs convert an incident photon into an electrical current pulse large enough to be detected by sensitive electronics (see SENSORS, OPTICAL). Other possibilities of detectors for lidar systems include multianode PMTs [18], avalanche photodiodes [19, 20], and charge-coupled devices (CCDs) [21, 22]. Coherent detection is discussed in Sect. 6.1.

The output of a PMT is in the form of current pulses that are produced both by photons entering the PMT as well as the thermal emissions of electrons inside the PMT, called *dark current*. The dark current is manifested as a background on the measured backscattered laser light.

There are two ways in which the output of a PMT can be recorded electronically. In one method, photon counting, the electrical pulses due to individual photons are counted; in the other technique, analog detection, the average current due to the PMT output pulses is measured and recorded. The most appropriate method to use depends on the average rate at which output pulses are produced.

3.3.1 Photon Counting

Photon counting is a two-step process. Firstly, the output of the PMT is filtered using a discriminator to remove a substantial number of the dark counts. Dark counts arise because of the thermal emission of electrons inside the PMT. These thermal

emissions occur throughout the PMT and the location of the electron emission determines the gain it experiences before appearing as a pulse at the PMT output. This average dark-count gain will be less than the average photon-induced gain, that is, the average dark-count pulse amplitude is less than the average photon-induced pulse amplitude. This allows the use of a discriminator that selectively passes pulses that have amplitude greater than some preset level. A properly adjusted discriminator significantly increases the ratio of signal-to-dark counts in the pulse stream from the PMT.

The second step in the photon-counting process is counting of the electrical pulses; this is typically achieved using a Multichannel scaler (MCS). An MCS has a number of memory locations that become active sequentially, and for a fixed amount of time after the laser is fired. Each time a photon is detected, the number in the currently active memory location is incremented by 1. In this way, each memory location represents a measurement range bin, Fig. 5.

When the incident light is sufficiently intense that the electrical pulses output by the PMT start to significantly overlap, and as overlapping pulses are difficult to distinguish from individual pulses, photon counting becomes ineffective and analog detection becomes more appropriate.

3.3.2 Analog Detection

Analog detection is appropriate when the average count rate approaches the pulse-pair resolution of the detector system, usually on the order of 10 to 100 MHz depending on the PMT type and the speed of the discriminator and the MCS. Analog detection systems use a fast analog-to-digital converter to convert the average current from the PMT into digital form suitable for recording and manipulation on a computer. The digital-to-analog conversion must be done at a rate capable of giving the range resolution required in the measurements.

3.4 An Example of a Lidar Detection System

The Purple Crow Lidar [23, 24] at the University of Western Ontario detects scattering at four wavelengths, Fig. 6. An Nd:YAG laser operating at the second-harmonic frequency (532 nm) provides the light source for the Rayleigh (532 nm) and the two Raman shifted channels, N_2 (607 nm) and H_2O (660 nm). The fourth channel is a sodium resonance–fluorescence channel that operates at 589 nm. Dichroic mirrors are used to separate light collected by the parabolic mirror into the four channels before being filtered by narrowband interference filters and directed onto the PMTs.

A rotating chopper is incorporated into the two high signal level channels (Rayleigh and sodium) to protect these PMTs from the intense near-field returns. The chopper comprises a rotating disk that has two teeth on the periphery; it rotates at 8400 rpm. The chopper is synchronized with the transmission of the laser pulses so

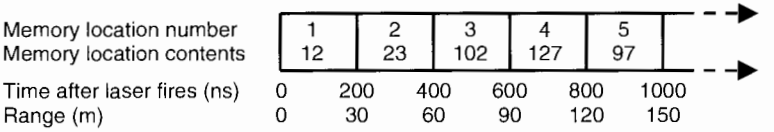

Fig. 5 Schematic of MCS operation

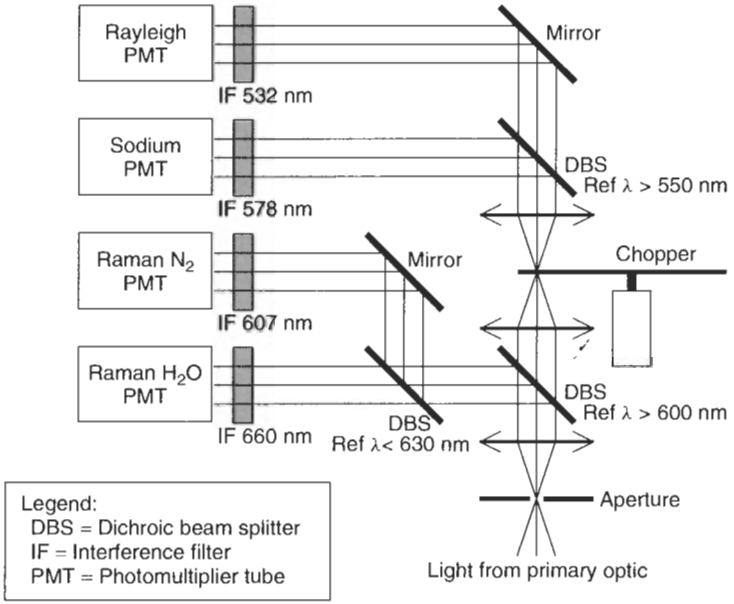

Fig. 6 The University of Western Ontario's Purple Crow Lidar detection system

that scatter from below 20 km is blocked, however, the shutter is fully open by the time light scattered from 30 km returns to the instrument.

The two Raman channels are used for the detection of H_2O and N_2 in the troposphere and stratosphere, allowing water vapor concentration and temperature profiles to be measured. Measurements from the Rayleigh and sodium channels are combined to provide temperature profiles from 30 to 110 km.

4 Rayleigh Lidar

Rayleigh theory [25, 26] describes the scattering of light by particles that are small compared to the wavelength of the incident radiation and is applicable to the elastic scattering of light by atmospheric molecules (see also RADIATION INTERACTION WITH MOLECULES). The intensity of Rayleigh-scattered light is proportional to the density of the atmosphere and as the atmospheric temperature is related to density, the temperature can be determined from measurements of the intensity of the Rayleigh backscatter profile.

Rayleigh lidar is the name given to a class of lidar systems that measure the intensity of the Rayleigh backscatter from about 30 km up to around 80 or 100 km. The principle of operation of a Rayleigh lidar system is straightforward. A pulse of laser light is fired up into the atmosphere and any photons that are backscattered and collected by the receiving system are counted as a function of range. The measured Rayleigh backscatter intensity profile can be used to determine a relative density profile; absolute calibration of a Rayleigh lidar is difficult, due in part to the uncertainty in the transmission of the lower atmosphere. The relative density profile can be used to determine an

absolute temperature profile by assuming that the atmosphere is in hydrostatic equilibrium and by applying the Ideal Gas Law. Details of the calculation and an error analysis for this technique can be found in both [27] and [28].

At altitudes below about 30 km, light is elastically scattered by aerosols in addition to the Rayleigh scattering from molecules; this scattering from aerosols contaminates the Rayleigh signal and sets the lower altitude limit for the application of the Rayleigh lidar. High spectral resolution techniques can be used to separate the scattering from these two sources [29].

The upper altitude limit for the Rayleigh lidar depends on the power of the lidar and the optical transmission of the lower atmosphere. Above about 90 km, the atmospheric density is extremely low resulting in low signal levels. Low signal levels give rise to large statistical uncertainties in the derived temperatures at the very top of the derived temperature profiles; at some point, the uncertainties become so large that the derived temperatures are not useful.

Rayleigh lidar systems are unable to operate when clouds obscure the middle atmosphere from their view. Additionally, most Rayleigh systems are able to operate only at nighttime due to the overwhelming presence of scattered solar photons during the day. However, the addition of an appropriately narrow band-pass filter in the receiver optics allows daytime measurements [30].

5 Aerosol Lidar

The theory of scattering that was developed by Mie early this century is a general solution that covers the scattering of electromagnetic radiation by homogeneous spheres of all sizes and refractive indices.

The atmosphere contains particles with an infinite variety of shapes, sizes, and refractive indices, usually referred to as aerosols. The measurement of the properties of atmospheric aerosols is complicated by the small size and the fragility of these particles. The processes of evaporation, condensation, coagulation, absorption, desorption, and chemical reactions serve to change the atmospheric aerosol composition on short timescales. Care must be taken with direct sampling methods in order that the sampling process allows correct interpretation of the properties of the collected aerosols.

Aerosol concentrations in the atmosphere vary widely with altitude, time, and location; they also play an important role in the radiation budget of the earth by scattering and absorbing both incoming solar radiation and outgoing terrestrial radiation. Climate models require detailed information on the optical properties, as well as the spatial and temporal distribution of atmospheric aerosols. Typically, the aerosol concentration decreases with increasing altitude throughout the troposphere, however, there is a layer of aerosols in the atmosphere from about 15 to 23 km. This is known as the stratospheric aerosol layer or the Junge [31] layer. The aerosols in this layer are primarily volcanic in origin and lidar measurements have shown that the altitude range and density of the aerosols in this layer vary widely depending on recent volcanic activity [32].

Since the early 1960s, a large number of lidars have been used to study aerosols and clouds in the troposphere and lower stratosphere. Instruments using multiple wavelength transmitters and receivers

as well as polarization techniques have been used to help quantify aerosol properties [33]. Lidars have been used to study polar stratospheric clouds (PSCs) [34, 35], to help understand the role they play in ozone depletion.

In September 1994, NASA flew a space shuttle mission, STS-64, which included the LITE experiment [36–38]. LITE was initially intended to serve as a technology development and validation exercise for future space lidar missions, however, it produced scientifically significant results [39, 40]. LITE incorporated an Nd:YAG laser operating simultaneously at three frequencies, the fundamental (1064 nm), the second harmonic (532 nm), and the third harmonic (355 nm). It also incorporated a system for automatic alignment of the laser beam into the FOV of the detector system.

6 Doppler Effects and Wind Lidar

Both random thermal motions and bulk mean flow (i.e., wind) contribute to the motion of the molecules and aerosols in the atmosphere. When a photon is scattered by a molecule or aerosol, it will suffer a change in frequency proportional to the component of its velocity in the direction of the laser beam, that is, line-of-sight (LOS) velocity, due to the Doppler effect.

Atmospheric aerosols have the same average velocity as atmospheric molecules as both types of scatterers are carried about by the wind, so that the average Doppler shift of the scattered light will be the same for scattering from both molecules and aerosols. The thermal velocity of molecules is much greater than that of aerosols due to their mass difference; this leads to the spectrum of the backscattered light having a distribution as shown in Fig. 7. The difference in the thermal (random) speeds of the molecules and aerosols leads to the two distinct regions of this distribution. The faster moving molecules result in a significantly wider spectral distribution than that due to aerosols [41, 42].

High spectral resolution measurements of backscattered light, in principle, allow the determination of LOS wind speed (from the frequency offset of the backscatter), the temperature (from the width of the molecular scattering function), and the separation of the signal due to molecules from that due to aerosols. In practice, making these high spectral resolution measurements with useful SNR is difficult, especially at large distances. However, several useful lidar techniques based on the measurement of Doppler shifts have been developed.

Separation of molecular and aerosol scattering is not necessary if only wind is to be measured since the average Doppler shift is the same for both molecular and aerosol scattering. The incoherent or direct detection wind lidar measures the LOS wind speed using optical techniques to

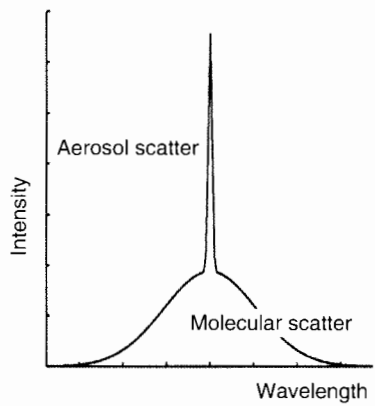

Fig. 7 Modeled spectrum of monochromatic light scattered by the atmosphere

measure the spectrum of the backscattered light and the transmitted laser. The Doppler shift and LOS wind speed are calculated from the measured spectral information. Incoherent wind lidar has been applied to the measurement of wind fields in the stratosphere [43] and the troposphere [44], however, coherent detection techniques (Sect. 6.1) are more commonly used in the troposphere.

In principle, it is possible to determine atmospheric temperature by measuring the spectral shape of the light backscattered from air molecules in the middle atmosphere. However, using this Doppler technique, the SNR requirements for temperature measurement is much higher than that for measuring winds [45]. In practice, Rayleigh–Doppler temperature measurements are quite difficult. The advantage of this method of temperature determination is that the true kinetic temperature of the atmosphere is obtained without the need for the assumptions required by the Rayleigh lidar technique.

6.1 Coherent Doppler Lidar

Coherent detection is used in a class of lidar designed for remote velocity measurement. This detection technique mixes the backscattered laser light with light from a local oscillator on a photomixer. The output of the photomixer is a radio frequency (RF) signal whose frequency is the difference between the frequencies of the two optical signals. Standard RF techniques are used to measure and record the photomixer output. The frequency of the measured RF signal can be used to determine the Doppler shift of the scattered laser light, which in turn allows the determination of the wind velocity [46].

Coherent lidar has more critical signal level requirements than the incoherent lidar. An incoherent lidar can make average measurements over an extended period of time to increase the SNR of the measurements. Although this decreases the temporal resolution of the measurements, this type of averaging cannot be applied to the coherent lidar in which a certain minimum signal level must be maintained to ensure valid measurements. With greater signal levels available in the lower atmosphere due to scattering from aerosols, the measurement of the Doppler shift via coherent detection becomes practical. Coherent Doppler lidar is used extensively in wind field mapping from the ground [47] and from the air [48]. There has been a great deal of interest in providing global tropospheric wind field maps based on space-based Doppler lidar systems; numerous studies [49] of both coherent and incoherent techniques have been undertaken in order to determine the best technique for this measurement.

7 Differential Absorption Lidar (DIAL)

In 1964, Schotland [50] suggested a new lidar technique that has become known as the differential absorption lidar (DIAL). This technique finds application in measuring the concentration of trace species in the atmosphere, in particular, pollutants and other chemically important minor constituents. The DIAL technique takes advantage of the sharp variation in optical transmission of the atmosphere near the absorption line of an atomic or molecular species. A DIAL transmits two closely spaced wavelengths – one coincides with an absorption line of the constituent of interest (λ_{on}), while the other is in the wing

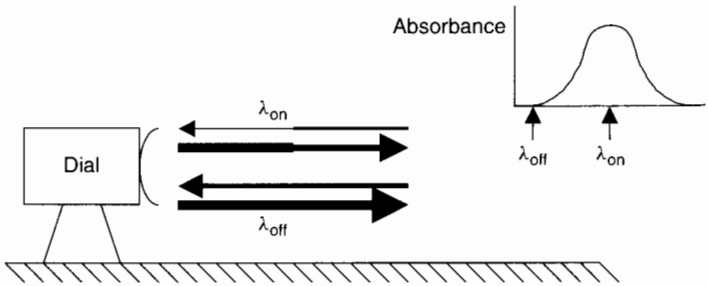

Fig. 8 Operation of a differential absorption lidar (DIAL)

of this absorption line (λ_{off}), Fig. 8. During transmission of these two wavelengths through the atmosphere, the emission that is tuned to the absorption line will suffer greater attenuation than the emission in the wing of the line. The backscattered intensity at the two wavelengths can be used to determine the optical attenuation due to the species and thus the concentration of that species. A DIAL can transmit the two wavelengths simultaneously, or alternate pulses of the two frequencies. Whichever scheme is used, it is necessary to ensure that the system efficiency is the same at both wavelengths, or is well quantified.

The first use of a DIAL system was for the measurement of atmospheric water vapor concentration [51]. The DIAL technique has been extensively used for pollution monitoring in the lower regions of the atmosphere; it has been used for the detection of a number of species including NO, O_3, SO_2, and CH_4. An important application of DIAL has been the measurement of ozone profiles in the middle atmosphere [52, 53]. Traditional methods for measuring ozone give the amount of ozone integrated over the entire depth of the atmosphere; the DIAL technique gives height profiles of ozone concentration.

Temperature measurement with DIAL is possible when an absorption line has a temperature dependence, this technique has found limited applications in the atmosphere [54, 55].

8 Raman Lidar

When monochromatic light, or light of sufficiently narrow spectral width, is scattered by a molecular gas or liquid, the spectrum of the scattered light contains lines at wavelengths different from that of the incident radiation [56]. First observed by Raman [57], this effect is due to the interaction of the radiation with the quantized vibrational and rotational energy levels of the molecule (see also SPECTROSCOPY, RAMAN). Raman scattering involves a transfer of energy between the incident light and the molecule and is therefore an inelastic process. The cross sections due to Raman scattering are included by the Rayleigh scattering theory [58], although Raman spectroscopists use the term Rayleigh line to indicate only the elastically scattered central component of the scattered light. The intensity of the most intense vibrational shifted Raman lines is typically a factor of about 1000 lower than that for the elastic scattering by molecules; this varies somewhat from molecule to molecule. The spectral shift for vibrational Raman scattering is

typically several hundred to a few thousand wave numbers. When scattering is accompanied by a change in the rotational state of the molecule only, pure rotational Raman lidar (PRRL), the scattered intensity is much greater, however, the spectral shift is much less, typically several to a few tens of wave numbers.

Each type of molecule has unique vibrational and rotational quantum energy levels and therefore, Raman scattering from each type of molecule has a unique spectral signature associated with these energy levels. This allows the presence of molecules to be determined by their scattered light spectra. Typically, the term *Raman lidar* refers to a lidar that makes use of a change in the vibrational state of the scattering molecule; this gives a much greater spectral shift in the scattered light than a change in the rotational state alone.

In the mid 1960s, Cooney [59] and Leonard [60] demonstrated the measurement of the Raman shifted light from nitrogen molecules in the troposphere by lidar. The Raman lidar has been most often applied to the measurement of atmospheric water vapor profiles [61, 62]. The determination of water vapor profiles is achieved by measuring the intensity of the light backscattered by both water vapor and nitrogen molecules, see Fig. 6. The measurement of the nitrogen Raman signal gives a reference that allows the absolute water vapor concentration to be determined. Raman lidar has also been applied to studying clouds [63]; there is a slight difference in the spectral signature of the scattering from the three phases of H_2O.

Raman lidar can be used to measure atmospheric temperature in two ways. As the vibrational Raman backscatter is spectrally distant from the scatter due to aerosols, the density profile of nitrogen can be measured. The mixing ratio of nitrogen in the atmosphere is a constant, except in the upper atmosphere; this allows the application of the Rayleigh lidar technique described above for the determination of temperature profiles. The Raman nitrogen signal is influenced by the presence of aerosols in that they affect the transmission of the atmosphere; this limits the application of this technique to the stratosphere and tropopause [64]. Aerosol concentrations in this region are typically relatively low and predictable, except after major volcanic events.

A second method of atmospheric temperature measurement utilizes the temperature dependence of the shape of the envelope of the pure rotational Raman spectrum [65]. High spectral resolution measurements allow the shape of the pure rotational Raman spectrum of air (effectively just nitrogen and oxygen) to be determined sufficiently well such that the temperature of the scatterers can be determined. As there is only a very small separation between the Raman pure rotational lines and the elastic scatter, careful attention must be paid to the effective separation of these signals in this technique [66].

9 Resonance Lidar

Resonant scattering occurs when the energy of an incident photon is equal to the energy of an allowed transition within an atom. This is an elastic process in which the atom absorbs the incident photon and instantly emits another photon at the same frequency. In general, the emitted photon will suffer a Doppler shift,

however, the scatterer will not undergo a change in its internal energy level, that is, it is an elastic process. The fluorescence spectrum is unique to a particular atomic or molecular species. This can be used to identify and measure the concentration of a particular species [67, 68].

The constant ablation of meteors in the earth's upper atmosphere leads to the existence of extended layers of a variety of alkali metals in the 80 to 115 km region. While the concentration of these metals is low, their resonant-scattering cross sections are quite high. For instance, at 589 nm, the resonance–fluorescence cross section for sodium is about 10^{15} times larger than the cross-section for Rayleigh scattering from air. This large cross section allows these metals to be fairly easily exploited by ground-based lidars.

The atmospheric sodium layer is the most widely probed of the atmospheric alkali metal layers using lidar. The sodium abundance is relatively high and the transmitter frequency is relatively easy to generate.

The spectral shape of the sodium line at 589 nm, the D_{2a} line, is temperature-dependent and the scattering cross section is proportional to the line shape. This allows the temperature of the sodium atoms and the atmosphere surrounding them to be determined from the spectral shape of the backscattered intensity. The measurement of the sodium D_{2a} shape has been achieved by lidar in a number of ways [69, 70]. Usually, this measurement is achieved by transmitting narrow bandwidth laser pulses at two or three well-known frequencies within the sodium D_{2a} line and recording the backscatter intensity at each of the transmitted frequencies separately. By knowing the frequency of the transmitted laser pulses and the intensity of the backscatter at each of the transmitted frequencies, the atmospheric temperature can be determined.

Resonance lidar temperature measurement is a direct spectral measurement and has associated uncertainties that are several orders of magnitude lower than those associated with Rayleigh temperature measurements in this altitude range.

Other alkali metals, including calcium [71], potassium [72], lithium [73], and iron [74] have also been used to study the mesopause region of the earth's atmosphere. Thomas [75] provides a review of the early work in this field. Resonance lidar requires laser transmissions at the precise frequency of the fluorescence line of the species being studied. Traditionally, dye lasers have been successfully used to probe many of these species, though working with these dyes is difficult in the field environment. Recently, solid-state lasers have been applied to resonance lidar systems [76].

Wind measurements are possible using a Na lidar. Transmission of laser pulses that are referenced to very narrow spectral features within the Na D_{2a} line allow the Doppler shift of the backscattered light and hence, the LOS wind speed to be determined [77].

10 Future

Lidar has established itself as one of the most important measurement techniques for atmospheric composition and dynamics from the surface to the upper atmosphere. It also has important uses in mapping, bathymetry, defense, oceanography, and natural resource management. Lidar solutions offer themselves to a wide range of environmental monitoring problems.

The technologies required for lidar are now mature enough that the past promises of global environmental monitoring by lidar are being fulfilled. Following two early space-based lidar systems – the French instrument ALISSA [78] on board the MIR platform and LITE [36] on the space shuttle, several space-based lidar systems are being planned, developed, or in operation. These include GLAS [79] for precision surface topography as well as cloud and aerosol studies, AMD-aelous [80] for global wind field measurement, the Vegetation Canopy Lidar [81] for measurements of the vegetation canopy and Earth surface topography, CALIPSO [82] to measure aerosols and clouds for climate studies, and MOLA [83], which has been used to measure the topography of Mars.

Another area where lidar has significant future potential is in digital 3-D imaging [84], particularly for including real objects, such as buildings, in virtual reality environments.

As technologies related to lidar such as laser and detector technologies develop further, lidar will continue to find application in a variety of remote sensing applications.

Glossary

Lidar: Light detection and ranging.

DIAL: Differential absorption lidar.

Active Remote Sensing: A technique that transmits radiation that interacts with the object under study. A fraction of the radiation is returned to the instrument for analysis.

Range: Distance from lidar to object/region being monitored.

Bistatic: Lidar with the transmitter and receiver separated by a distance not insignificant compared to the operating range.

Monostatic: Having the transmitter and receiver colocated, that is, separated by a small distance compared to the operating range.

Biaxial: Having two axes; the optical axis of the transmitter is different from that of the receiver.

Coaxial: Having a single axis; the optical axis of the transmitter is coincident with that of the receiver.

Bathymetry: Water depth measurement, usually in coastal regions and in lakes.

PRF: Pulse-repetition frequency: the rate at which a laser produces output pulses.

Middle Atmosphere: The region of the atmosphere from about 10 km to about 100 km.

Troposphere: The region of the atmosphere from the ground to about 10 km varies with latitude and season. This region contains weather phenomena.

Stratospheric Aerosol Layer: A layer of aerosol (particulates) in the lower stratosphere (15 to 25 km) primarily volcanic in origin.

Raman Lidar: Lidar that uses the Raman component of the backscattered light.

Doppler Lidar: Lidar that measures wind and/or temperature based on the Doppler shift of the backscattered light.

LOS: Line of sight. Wind lidar typically measures the component of the wind velocity in the direction of the transmitted laser beam.

PRRL: Pure rotational Raman lidar: a lidar that utilizes the pure rotational part of the Raman scatter.

References

[1] Synge, E. H. (**1930**), *Philos. Mag.* **52**, 1014–1020.
[2] Duclaux (**1936**), *J. Phys. Radiat.* 7, 361.
[3] Hulbert, E. O. (**1937**), *J. Opt. Soc. Am.* **27**, 377–382.
[4] Bureau, R. (**1946**), *Meteorologie* **3**, 292.
[5] Friedland, S. S., Katzenstein, J., Zatzick, M. R. (**1956**), *J. Geophys. Res.* **61**, 415–434.
[6] Maiman, T. H. (**1960**), *Nature* **187**, 493.
[7] McClung, F. J., Hellworth, R. W. (**1962**), *J. Appl. Phys.* **33**, 828–829.
[8] Smullins, L. D., Fiocco, G. (**1962**), *Nature* **194**, 1267.
[9] Beneditti-Michelangeli, G., Congeduti, F., Fiocco, G. (**1972**), *JAS* **29**, 906–910.
[10] Abreu, V. J., Barnes, J. E., Hays, P. B. (**1992**), *Appl. Opt.* **31**, 4509–4514.
[11] Shipley, S. T., Tracey, D. H., Eloranta, E. W., Trauger, J. T., Sroga, J. T., Roesler, F. L., Weinman, J. A. (**1983**), *Appl. Opt.* **22**, 3716–3724.
[12] Fiocco, G., DeWolf, J. B. (**1968**), *JAS* **25**, 488–496.
[13] Chanin, M. L., Garnier, A., Hauchecorne, A., Porteneuve, J. (**1989**), *J. Geophys. Res.* **16**, 1273–1276.
[14] Carswell, A. I. (1983), in D. A. Killinger, A. Mooradian (Ed.), *Optical and Laser Remote Sensing*. Berlin: Springer-Verlag, pp. 318–326.
[15] Sassen, K., Benson, R. P., Spinhirne, J. D. (**2000**), *Geophys. Res. Lett.* **27**, 673–676.
[16] Cairo, F., Congeduti, F., Poli, M., Centurioni, S., DiDonfrancesco, G. (**1996**), *Rev. Sci. Instrum.* **67**, 3274–3280.
[17] Williamson, C. K., De Young, R. J. (**2000**), *Appl. Opt.* **39**, 1973–1979.
[18] McGill, M. J., Skinner, W. R. (**1997**), *Opt. Eng.* **36**, 139–145.
[19] Maruyama, T., Narusawa, F., Kudo, M., Tanaka, M., Saito, Y., Nomura, A. (**2002**), *Opt. Eng.* **41**, 395–402.
[20] Spinhirne, J. D. (**1993**), *IEEE Trans. Geosci. Remote Sens.* **31**, 48–55.
[21] Irgang, T. D., Hays, P. B., Skinner, W. R. (**2002**), *Appl. Opt.* **41**, 1145–1155.
[22] South, A. M., Povey, I. M., Jones, R. L. (**1998**), *J. Geophys. Res.* **103**, 31191–31202.
[23] Sica, R. J., Sargoytchev, S., Argall, P. S., Borra, E. F., Girard, L., Sparrow, C. T., Flatt, S. (**1995**), *Appl. Opt.* **34**, 6925–6936.
[24] Argall, P. S., Vassiliev, O. N., Sica, R. J., Mwangi, M. M. (**2000**), *Appl. Opt.* **39**, 2393–2400.
[25] Rayleigh, (J. W. Strutt) (**1871**), *Philos. Mag.* **41**, 274–279.
[26] Rayleigh, (J. W. Strutt) (**1871**), *Philos. Mag.* **41**, 447–454.
[27] Hauchecorne, A., Chanin, M. L. (**1980**), *Geophys. Res. Lett.* 7, 565–568.
[28] Shibata, T., Kobuchi, M., Maeda, M. (**1986**), *Appl.Opt.* **25**, 685–688.
[29] Fiocco, G., Beneditti-Michelangeli, G., Maischberger, K., Madonna, E. (**1971**), *Nature* **229**, 79–80.
[30] Gille, S. T., Hauchecorne, A., Chanin, M. L. (**1991**), *J. Geophys. Res.* **96**, 7579–7587.
[31] Junge, C. E. (1963), *Air Chemistry and Radioactivity*. New York: Academic Press.
[32] McCormick, M. P., Swissler, T. J., Chu, W. P., Fuller Jr, W. H. (**1978**), *J. Atmos. Sci.* **35**, 1296–1303.
[33] Reagan, G. A., Spinhirne, J. D., McCormick, M. P. (**1989**), *Proc. IEEE* 77, 433–448.
[34] Donovan, D. P., Fast, H., Makino, Y., Bird, J. C., Carswell, A. I., Davies, J., Duck, T. J., Kaminski, J. W., McElroy, C. T., Mittermeier, R. L., Pal, S. R., Savastiouk, V., Velkov, D., Whiteway, J. A. (**1997**), *Geophys. Res. Lett.* **24**, 2709–2712.
[35] Stefanutti, L., Morandi, M., Delguasta, M., Godin, S., Megie, G., Brechet, J., Piquard, J. (**1991**), *J. Geophys. Res.* **96**, 12975–12987.
[36] http://oea.larc.nasa.gov/PAIS/LITE.html.
[37] Winker, D. M., Couch, R. H., McCormick, M. P. (**1996**), *Proc. IEEE* **84**, 164–180.
[38] O'Connor, L. (**1995**), *Mech. Eng.* **117**, 77–79.
[39] Omah, A. H., Gardner, C. S. (**2001**), *J. Geophys. Res.* **106**, 1227–1236.
[40] Winker, D. M., Trepte, C. R. (**1998**), *Geophys. Res. Lett.* **25**, 3351–3354.

[41] Fiocco, G., Benedetti-Michelangeli, G., Maischberger, K., Madonna, E. (**1971**), *Nature* **229**, 79–80.
[42] Shimizu, H., Lee, S. A., She, C. Y. (**1983**), *Appl. Opt.* **22**, 1373–1382.
[43] Tepley, C. A., Sargoytchev, S. I., Hines, C. O. (**1991**), *Geophys. Res. Lett.* **18**, 167–170.
[44] Abreu, V. J., Barnes, J. E., Hays, P. B. (**1992**), *Appl. Opt.* **31**, 4509–4514.
[45] Tepley, C. A., Sargoytchev, S. I., Rojas, R. (**1993**), *IEEE Trans. Geosci. Remote Sens.* **31**, 36–47.
[46] Frehlich, R. (1976), in A. Consortini (Ed.), *Trends in Optics*. London: Academic Press.
[47] Hardesty, R. M. (1983), in D. K. Killinger, A. Mooradian (Eds.), *Optical and Laser Remote Sensing*. Berlin: Springer-Verlag.
[48] Bilbro, J., Fichtl, G., Fitzjarrald, D., Krause, M., Lee, R. (**1984**), *Bull. Am. Meteorol. Soc.* **65**, 348–359.
[49] Abreu, V. (**1979**), *Appl. Opt.* **18**, 2992–2997.
[50] Schotland, R. M. (1964), *Proc. of the Third Symposium on Remote Sensing of the Environment*, pp. 215–224.
[51] Schotland, R. M. (1966), *Proc. of the Fourth Symposium on Remote Sensing of the Environment*, pp. 273–283.
[52] Pelon, J., Godin, S., Megie, G. (**1986**), *J. Geophys. Res.* **91**, 8667–8671.
[53] McGee, T. J., Whiteman, D., Ferrare, R., Butler, J. J., Burris, J. F. (**1991**), *Opt. Eng.* **30**, 31–39.
[54] Browell, E. V., Ismail, S., Grossmann, B. E. (**1991**), *Appl. Opt.* **30**, 1517–1524.
[55] Theopold, F. A., Bosenberg, J. (**1993**), *J. Atmos. Ocean Tech.* **10**, 165–179.
[56] Herzberg, G. (1950), *Molecular Spectra and Molecular Structure I. Spectra of Diatomic Molecules*, (2nd ed.), New York: Van Nostrand Reinhold Company.
[57] Raman, C. V. (**1928**), *Indian J. Phys.* **2**, 387.
[58] Young, A. T. (**1981**), *Phys. Today* **35**, 42–48.
[59] Cooney, J. A. (**1968**), *Appl. Phys. Lett.* **12**, 40–42.
[60] Leonard, D. A. (**1967**), *Nature* **216**, 142–143.
[61] Cooney, J. A. (**1972**), *J. Geophys. Res.* **77**, 1078–1080.
[62] Melfi, S. H. (**1972**), *Appl.Opt.* **11**, 1605.
[63] Whiteman, D. N., Melfi, S. H. (**1999**), *J. Geophys. Res.* **104**, 31411–31419.
[64] Keckhut, P., Chanin, M. L., Hauchecorne, A. (**1990**), *Appl. Opt.* **29**, 5182–5186.
[65] Cooney, J. (**1971**), *J. Appl. Meteorol.* **11**, 108–112.
[66] Arshinov, Y., Bobrovnikov, S. (**1999**), *Appl. Opt.* **38**, 4635–4638.
[67] Chamberlain, J. W. (1961), *Physics of Aurora and Airglow*. New York: Academic Press.
[68] Measures, R. M. (1994), *Laser Remote Sensing: Fundamentals and Applications*. New York: John Wiley & Sons.
[69] Gibson, A., Thomas, L., Bhattacharyya, S. (**1979**), *Nature* **281**, 131–132.
[70] Frick, K. H., von Zahn, U. (**1985**), *J. Atmos. Terr. Phys.* **47**, 499–512.
[71] Granier, C., Jegou, J. P., Megie, G. (**1984**), *Geophys. Res. Lett.* **12**, 655–658.
[72] Megie, G., Bos, F., Blamont, J. E., Chanin, M. L. (**1978**), *Planet. Space Sci.* **26**, 27–35.
[73] Jegou, J. P., Chanin, M. L., Megie, G., Blamont, J. E. (**1980**), *Geophys. Res. Lett.* **7**, 995–998.
[74] Granier, C., Jegou, J. P., Megie, G. (**1989**), *Geophys. Res. Lett* **16**, 243–246.
[75] Thomas, L. (**1987**), *Philos. Trans. R.. Soc. London, Ser. A* **323**, 597–609.
[76] von Zahn, U., Hoffner, J. (**1996**), *Geophys. Res. Lett.* **23**, 141–144.
[77] Gardner, C. S., Tao, X., Papen, G. C. (**1995**), *Geophys. Res. Lett.* **22**, 2877–2880.
[78] Chanin, M. L., Hauchecorne, A., Malique, C., Nedeljkovic, D., Blamont, J. E., Desbois, M., Tulinov, G., Melnikov, V. (**1999**), *C R. Acad. Sci. II A* **328**, 359–366.
[79] http://glas.gsfc.nasa.gov/.
[80] http://www.esa.int/export/esaLP/aeolus.html.
[81] http://www.geog.umd.edu/vcl/.
[82] http://www-calipso.larc.nasa.gov/index.html.
[83] http://ltpwww.gsfc.nasa.gov/tharsis/mola.html.
[84] http://www.optech.on.ca/prodilris.htm.

Further Reading

Frehlich, R. (1996), in A. Consortini (Ed.), *Trends in Optics: Research, Development and Applications*. London, UK: Academic Press, pp. 351–370.
Grant, W. B. (1995), in F. J. Duarte (Ed.), *Tunable Laser Applications*. New York: Marcel Dekker, pp. 213–305.

Killinger, D. K., Mooradian, A. (Ed.) (1983), *Optical and Laser Remote Sensing*. Berlin: Springer-Verlag.

Measures, R. M. (1984), *Laser Remote Sensing: Fundamentals and Applications*. New York: John Wiley & Sons.

Singh, U. H. (1997), in P. K. Rastogi (Ed.), *Optical Measurement Techniques and Application*. Norwood, MA: Artech House, pp. 369–396.

Thomas, L. (1995), in R. J. H. Clark, R. E. Hester (Eds.), *Spectroscopy in Environmental Science*. Chichester, UK: John Wiley & Sons, pp. 1–47.

Weitkamp, C. (1996), in E. Raschke (Ed.), *Radiation and Water in the Climate System*. Berlin, Germany: Springer-Verlag, pp. 217–247.